Available online at www.sciencedirect.com
SCIENCE DIRECT®
ELSEVIER
Journal of Nuclear Materials 329–333 (2004) 687–691
journal of nuclear materials
www.elsevier.com/locate/jnucmat

High heat flux properties of pure tungsten and plasma sprayed tungsten coatings

X. Liu [a,*], S. Tamura [b], K. Tokunaga [b], N. Yoshida [b], N. Noda [c], L. Yang [a], Z. Xu [a]

[a] Southwestern Institute of Physics, P.O. Box 432, Chengdu 610041, Sichuan, China
[b] Research Institute for Applied Mechanics, Kyushu University, 6-1 Kasugakoen, Kasuga, Fukuoka 816-8580, Japan
[c] National Institute for Fusion Science, Toki, Gifu 509-5292, Japan

Abstract

High heat flux properties of pure tungsten and plasma sprayed tungsten coatings on carbon substrates have been studied by annealing and cyclic heat loading. The recrystallization temperature and an activation energy $Q_R = 126$ kJ/mol for grain growth of tungsten coating by vacuum plasma spray (VPS) were estimated, and the microstructural changes of multi-layer tungsten and rhenium interface pre-deposited by physical vapor deposition (PVD) with anneal temperature were investigated. Cyclic load tests indicated that pure tungsten and VPS-tungsten coating could withstand 1000 cycles at 33–35 MW/m^2 heat flux and 3 s pulse duration, and inert gas plasma spray (IPS)-tungsten coating showed local cracks by 300 cycles but did not induce failure by further cycles. However, the failure of pure tungsten and VPS-tungsten coating by fatigue cracking was observed under higher heat load (55–60 MW/m^2) for 420 and 230 cycles, respectively.

1. Introduction

Both tungsten and tungsten coating are considered as the armour materials for the divertor of ITER, they can be prepared by powder metallurgy (PM) and by chemical vapor deposition (CVD) or plasma spray (PS). The interactions of tungsten with plasma have being studied in some fusion devices, for example, TEXTOR [1] and ASDEX-Upgrade [2], or by the laboratory simulations [3,4], and special attention is paid to its high heat flux removal properties, such as thermo-mechanical, structural stability and thermal fatigue resistance properties.

In the present experiment, PM-W and PS-W coatings were used and their high heat flux removal properties were investigated, of which tungsten coated carbon/carbon fiber composite (CFC) CX-2002U by vacuum plasma spray (VPS) has multi-layer W, Re interfaces pre-deposited by physical vapor deposition (PVD). Previous researches indicated that this W, Re multi-layer kept its original structure at 1300 °C but the multi-layer structure completely disappeared at a peak temperature of about 2800 °C [5,6]. However, detailed changes of the multi-layer W, Re structure at elevated temperature were not completely clear. Therefore, in this work, the recrystallization and microstructural changes of this VPS-W coating were investigated, and then the thermal fatigue experiments of PM-W and VPS-W/CFC were performed with an electron beam. For comparison, tungsten coated graphite by inert gas plasma spray (IPS) was also tested.

2. Experimental

The VPS-W coating is 0.5 mm thickness and with an interface of W and Re layers alternately deposited by PVD [5]. The density of tungsten coating is 92.5% of the

* Corresponding author. Tel.: +86-28 8293 2227; fax: +86-28 8293 2202.
E-mail address: xliu@swip.ac.cn (X. Liu).

0022-3115/$ - see front matter
doi:10.1016/j.jnucmat.2004.04.217

theoretical value. Heat treatment was performed at 1000 °C for several hours to stabilize its microstructure. Tungsten coated SMF 700 graphite (from China) by inert gas plasma spray (IPS-W/C) was also prepared and has the same thickness but with a higher porosity (∼16%). The size of both VPS-W/CFC and IPS-W/C specimens is 10×10×5 mm. Pure tungsten specimens with size of 10×10×2.5 mm were cut from a hot-rolled tungsten plate and have 99.95% purity (from Northwest Institute of Non-Ferrous Metals, China).

The anneal and cyclic load experiments were carried out by an electron beam, the specimens were fixed mechanically on a copper sink actively cooled by water, the surface temperature of specimens was measured by two-color optical pyrometers which were calibrated by thermocouple before measurements. The grain sizes, surface modifications of tested specimens were observed by scanning electron microscopy (SEM) and the compositions were measured by X-ray energy diffraction spectroscopy (EDS).

3. Results and discussion

3.1. Recrystallization

In this work, VPS-W/CFC specimens were heated by an electron gun and isothermal and isochronal annealing were performed. Fig. 1 shows the relationship of grain sizes (average value comes from 20 samples) with anneal temperature and time. Based on this figure, the recrystallization temperature of VPS-W coating is estimated as 1400 °C, which is comparable with the conventional powder metallurgy (PM) tungsten.

Grain growth can be described by the Burke and Turnbull's equation [7]:

$$D^n - D_0^n = ct,$$

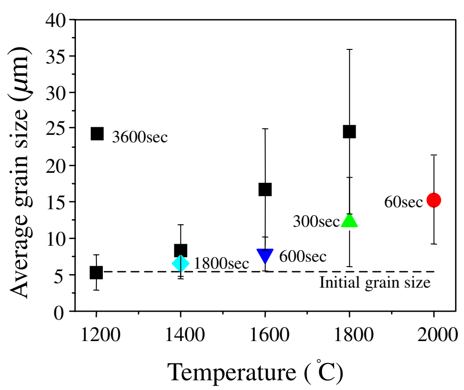

Fig. 1. Average grain size of VPS-W as a function of annealing temperature.

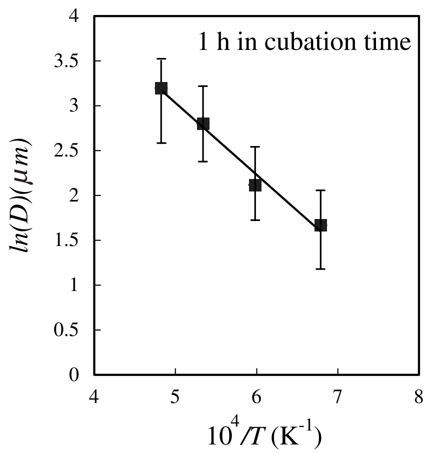

Fig. 2. Plot of ln(D) against 10^4 T^{-1}.

where the constant n, often termed grain growth exponent, usually equals 2 for pure metal, D, grain size, D_0, the initial grain size, t, the incubation time and c, rate constant. The rate constant depends on the annealing temperature in an Arrhenius form so that it is written as $c = c' \exp(-Q_R/RT)$, where c' is the pre-exponential term, R, gas constant, Q_R, the activation energy for grain growth and T, the absolute temperature of annealing. Taking the constant $n = 2$, the grain growth follows the expression

$$D^2 - D_0^2 = c' t \exp(-Q_R/RT).$$

The activation energy for grain growth may be deduced from this equation. Fig. 2 shows the plots of ln(D) against $10^4/T$ based on the data of isochronal annealing in Fig. 1, where a straight line can be drawn through data points and the slope of this line gives $Q_R/2R$ so that the activation energy for grain growth, Q_R, can be deduced to be $Q_R = 126$ kJ/mol.

3.2. Compositional changes of diffusion barrier

Anneal experiments resulted in not only grain growth but also the compositional changes of the coating, particularly for the multi-layer W, Re interface of VPS-W/CFC, so that the inherent characteristics of this diffusion barrier could be changed. Results indicated that the original structure of W, Re multi-layer (see Ref. [5]) did not change so much in the cases of 1200 °C anneal for 1 h and 1400 °C anneal for half an hour. However, the situation at the anneal temperature over 1400 °C was different, after annealing at 1600 °C for 10 min, for example, both image contrast and EDS line profile indicated that one tungsten layer had disappeared and the boundaries of W and Re layers became obscure as shown in Fig. 3(a), and finally, all the boundaries of W

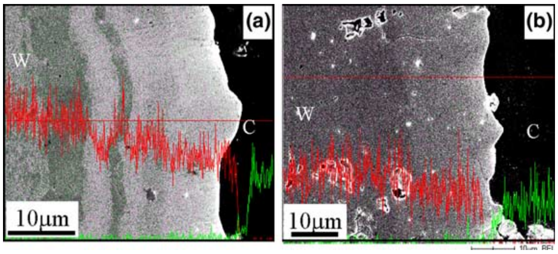

Fig. 3. Backscattering electron images of the polished cross-section of VPS-W/CFC after annealing at 1600 °C for 10 min (a) and 2000 °C for 1 min (b). EDS line profile of W and C was also included.

and Re layers pretty nearly disappeared by 2000 °C annealing for even just one minute (Fig. 3(b)). The main reason is due to mutual diffusion and solubility between W and Re. On the other hand, active carbon atoms will also diffuse towards Re and W layer during the annealing processes. As a result, the original function of the multi-layer W, Re structure as diffusion barrier will be changed and even failed. In fact, for 1 h incubation time, brittle tungsten carbides have been observed at the interface for the cases of higher than 1600 °C anneal temperature, in these cases the diffusion barrier has completely failed. Detailed investigation can be found in Ref. [8].

3.3. Cyclic load tests

Cyclic load tests were performed with a 60 keV electron beam with Gaussian-like distribution. In the present experiments, the diameter of electron beam was 4.5 mm and the average heat flux absorbed by specimens was estimated by measured current through the specimen. The pulse duration of electron beam is 3 s and the interval (30–60 s) is chosen to ensure that every cycle would cross the ductile-to-brittle transition temperature (DBTT) of tungsten, simulating the worst operation conditions of fusion devices.

In the first cyclic load experiment (Test I), the output power of electron gun was kept constant, the absorbed heat flux measured by current through the specimen was 33 and 35 MW/m^2, respectively for PM-W and PS-W coatings, and the corresponding surface temperature was 750–900 °C for VPS-W/CFC, 1500–1650 °C for IPS-W/C and 1000–1200 °C for PM-W. Heat transfer efficiency (power absorbed by the specimen divided by the power of electron gun) obtained in this case was 54–59% depending on surface emissivity. A similar heat transfer efficiency of about 53% has been reported for PS-W coating [3]. Usually surface emissivity depends on material, surface roughness and temperature. Therefore, there is a deviation between the absorbed heat flux of PM-W and PS-W coating, but no obvious deviation was found for IPS and VPS coating.

Surface temperature depends on the thermal conduction of specimens. Usually IPS coating has lower thermal conductivity than VPS coating, and the thermal conductivity of SMF 700 graphite (substrate material of IPS-W/C) is about 4 times lower than that of CX-2002U (substrate material of VPS-W/CFC) [9,10]. Therefore, a higher surface temperature was expected for IPS-W/C. Local cracks due to mechanical strain induced by heat loading were observed after 300 cycles at 35 MW/m^2 heat flux, most of which were parallel to the loaded surface owing to the lamellar structure of IPS coating and WC phase formed at the interface and caused a higher surface temperature (~2100 °C). However, further cycles did not induce obvious rise of the surface temperature, otherwise a stable surface temperature was observed from 300 to 400 cycles. Combining with surface topography observations by SEM, which shows crack propagation does not happen significantly, it indicates that the high porosity of IPS coating provides a crack-arresting mechanism, so that stresses arising in IPS coating during thermal load can be relieved by pores and crack propagation is restrained.

In the case of Test I, no visible damage was found on the surface of PM-W and VPS-W/CFC after 1000 cycles, indicating their perfect thermal fatigue resistance capabilities, at least under relatively low heat flux where the surface temperature is below the recrystallization temperature. Additionally, the grain boundaries of PM-W can be observed though not so clearer than the case of Test II. Similar phenomena have been reported when PM-W was heated at high temperature [11].

In the next cyclic load experiment (Test II), the absorbed heat flux of specimens was adjusted to obtain the same surface temperature (2000–2200 °C) for both PM-W and VPS-W/CFC. Obvious cracks were observed after 230 and 420 cycles, respectively at 60 MW/m^2 heat flux for VPS-W/CFC and 55 MW/m^2 heat flux for PM-W (pulse duration time was 3 s). Further cycles can more or less induce crack propagation. Fig. 4 shows the surface SEM photographs of VPS-W/CFC and PM-W specimens by 387 and 480 cycles, respectively. A crack appeared in the surface of both VPS-W/CFC and PM-W, it crossed the irradiation area and extended to the edges of the specimen for the former (see Fig. 4(c)), and for the latter it could be originated from one edge and extended gradually to the irradiation zone Fig. 4(a), moreover, this crack penetrated through the whole thickness of the PM-W specimen. The reason for this may be due to the defects on the edge of specimen during machining processes, which act as crack initiators. Almost all cracking is of intergranular nature as shown in Fig. 4(b) but the situation of intragranular fracture was also observed. In the case of VPS-W/CFC, one top of the crack ended at the zone with large pores and high porosity. By viewing the fracture surface as shown in Fig. 4(d), one can see that it seems to be characterized by

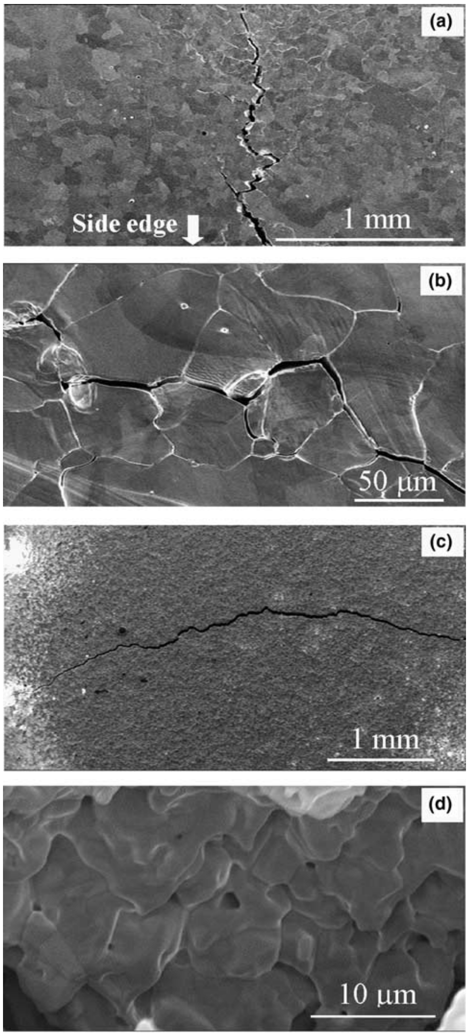

Fig. 4. SEM photographs of PM-W (a,b) after 480 cycles at 60 MW/m^2 heat flux and 3 s pulse length and VPS-W/CFC (c,d) after 387 cycles at 55 MW/m^2 heat flux and 3 s pulse length, where the surface temperature is 2000–2200 °C for both cases. The photograph (d) is the inside view of the crack in (c).

the debonding among sprayed tungsten particles. It is an indication that the formation of cracks results from the high residual stresses following spray processes and low strength, in particular the tensile strength, which is about 5–7 times smaller for PS-W coating than sintered tungsten [12]. Additionally, some small pores can be clearly seen on the fracture surface, but these pores are not enough to stop crack propagation. In the previous study [13], particle emission of VPS-W/CFC has been observed, but only the evaporation of PM-W was found under high heat loading. Based on the discussions above, PM-W seems to have better high heat flux removal properties than PS-W coating.

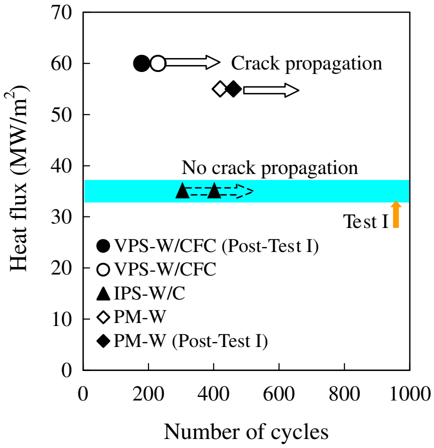

Fig. 5. A relationship of crack formation with heat flux and the number of cycles.

PM-W and VPS-W/CFC specimens survived 1000 cycles at 33 or 35 MW/m^2 without any damage (Test I). After following thermal cycling of Test II, cracks appeared in the surface of PM-W and VPS-W/CFC after 460 and 180 cycles, respectively, which did not show obvious difference compared with the un-irradiated specimens. Fig. 5 shows the relationship of crack formation and propagation with heat flux and the number of cycles. It can be seen that once cracks have been initiated, crack propagation will take place with further thermal cycles except the IPS-W coating. The reason is due to the high elastic strain energy stored within PM-W and VPS-W/CFC arising from thermal deformation during the heat load, which provides the driving force for crack propagation. Although relatively high porosity of PS coating may play the role of relieving stresses and limiting crack propagation, significant crack-arresting mechanism was found only in IPS coating owing to its higher porosity. Since high porosity is not expected for plasma facing materials, crack propagation in PM-W and VPS-W coating will be a crucial issue for their application as plasma facing materials.

4. Conclusions

Based on the investigation on the high heat flux removal properties of PM-W and PS-W coatings, results obtained in this study are summarized as follows:

1. The recrystallization temperature of VPS-W/CFC was about 1400 °C and an activation energy $Q_R =$ 126 kJ/mol for grain growth was estimated.
2. The microstructure of multi-layer W, Re interface will be changed by annealing processes and this multi-layer structure pretty nearly disappears by

2000 °C anneal for even just 1 min.The function of multi-layer W, Re interface as diffusion barrier will be completely failure by one hour anneal at the temperature over 1600 °C due to the formation of brittle tungsten carbides.
3. PM-W and VPS-W/CFC can withstand 1000 cycles at 33–35 MW/m^2 heat flux and 3 s pulse length, and local cracks appeared in the coating of IPS-W/C by 300 cycles, meanwhile the surface temperature jumped to a higher level owing to cracks parallel to the loaded surface. However, further cycles did not induce crack propagation due to crack-arresting mechanism of high porosity in IPS coating.
4. Cracks appeared in the surface of VPS-W/CFC and PM-W after 230 and 420 cycles, respectively at 55 and 60 MW/m^2 heat flux, where 2000–2200 °C surface temperature was obtained for both the specimens. Crack formation did not show significant difference for the specimens, which had experienced 1000 cycles at lower heat flux. Meanwhile crack propagation has been observed.

Acknowledgement

This work was partly supported by China–Japan Core University Program.

References

[1] T. Tanabe, M. Wada, T. Ohgo, V. Philipps, M. Rubel, A. Huber, J. Von Seggern, K. Ohya, A. Pospieszczyk, B. Schweer, J. Nucl. Mater. 283–287 (2000) 1128.
[2] K. Krieger, H. Maier, R. Neu, J. Nucl. Mater. 266–269 (1999) 207.
[3] M. Merola, I. Bobin-Vastra, A. Cardella, et al., Fus. Eng. Des. 49&50 (2000) 289.
[4] C. Garcia-Rosales, S. Deschka, W. Hohenauer, et al., Fus. Technol. 32 (1997) 263.
[5] K. Tokunaga, N. Yoshida, N. Noda, et al., J. Nucl. Mater. 266–269 (1999) 1224.
[6] K. Tokunaga, T. Matsubara, Y. Miyamoto, et al., J. Nucl. Mater. 283–287 (2000) 1121.
[7] G.F. Bolling, W.C. Winegard, Acta Met. 5 (1958) 283.
[8] S. Tamura, X. Liu, K. Tokunaga, Y. Tsunekawa, M. Okumiya, N. Noda, N. Yoshida, J. Nucl. Mater. these Proceedings. doi:10.1016/j.jnucmat.2004.04.186.
[9] X. Liu, Z.Y. Xu, J.M. Chen, L.W. Yan, Y. Liu, J. Nucl. Mater. 307–311 (2002) 84.
[10] I. Smid, M. Akiba, M. Araki, S. Suzuki, K. Satoh, Report JAERI-M, 93-149, 1993.
[11] D. Nishijima, M.Y. Ye, N. Ohno, S. Takamura, J. Nucl. Mater. 313–316 (2003) 97.
[12] B. Riccardi, A. Pizzuto, L. Bertamini, M. Diotallevi, G. Vieider, in: Proceeding of the SOFE-17, San Diego, CA, 6–9 October 1997, p. 910.
[13] X. Liu, N. Yoshida, N. Noda, F. Zhang, Z. Xu, Y. Liu, J. Nucl. Mater. 313–316 (2003) 399.